

Energy-dispersive x-ray diffraction and Raman scattering of Zn $1-x$ Mn x Se bulk crystals at high pressure

C. S. Yang, C. S. Ro, W. C. Chou, C. M. Lin, D. S. Chuu, J. Hu, E. Huang, and J. Xu

Citation: *Journal of Applied Physics* **85**, 8092 (1999); doi: 10.1063/1.370647

View online: <http://dx.doi.org/10.1063/1.370647>

View Table of Contents: <http://scitation.aip.org/content/aip/journal/jap/85/12?ver=pdfcov>

Published by the [AIP Publishing](#)

Articles you may be interested in

Local environment of a diluted element under high pressure: Zn $1-x$ Mn x O probed by fluorescence x-ray absorption spectroscopy

Appl. Phys. Lett. **89**, 231904 (2006); 10.1063/1.2400109

Effect of Mn composition on characterization of Zn $1-x$ Mn x S epilayers

J. Vac. Sci. Technol. A **23**, 777 (2005); 10.1116/1.1868592

Effect of Mn composition on characterization of Zn $1-x$ Mn x Se epilayers

J. Vac. Sci. Technol. A **22**, 1908 (2004); 10.1116/1.1705645

Synthesis, optical, and magnetic properties of diluted magnetic semiconductor Zn $1-x$ Mn x O nanowires via vapor phase growth

Appl. Phys. Lett. **83**, 4020 (2003); 10.1063/1.1625788

Curie temperature and carrier concentration gradients in epitaxy-grown Ga $1-x$ Mn x As layers

Appl. Phys. Lett. **82**, 3278 (2003); 10.1063/1.1573369



Re-register for Table of Content Alerts

Create a profile.



Sign up today!



Energy-dispersive x-ray diffraction and Raman scattering of $\text{Zn}_{1-x}\text{Mn}_x\text{Se}$ bulk crystals at high pressure

C. S. Yang, C. S. Ro, and W. C. Chou^{a)}

Department of Physics, Chung Yuan Christian University, Chung-Li 32023, Taiwan, Republic of China

C. M. Lin

Department of Mathematics and Science Education, National Hsinchu Teachers College, Hsinchu, Taiwan, Republic of China

D. S. Chuu

Department of Electro-physics, National Chiao Tung University, Hsin-Chu, Taiwan, Republic of China

J. Hu

Geophysical Laboratory, Carnegie Institution of Washington, DC 20015

E. Huang and J. Xu

Institute of Earth Sciences, Academia Sinica, Nan-Kang, P.O. Box 1-55, Taipei, Taiwan, Republic of China

(Received 19 June 1998; accepted for publication 17 March 1999)

Energy-dispersive x-ray diffraction experiments were carried out to investigate the structure of phase transitions under high pressure. It was found that the zinc blende (B_3) to rock salt (B_1) phase transition pressures of $\text{Zn}_{0.93}\text{Mn}_{0.07}\text{Se}$ and $\text{Zn}_{0.76}\text{Mn}_{0.24}\text{Se}$ bulk crystals are found 11.8 ± 1.5 and 9.9 ± 0.5 GPa, respectively. The respective bulk moduli are 61.8 ± 0.8 and 60.5 ± 0.8 GPa. The pressure-induced zinc blende (ZB) to rock salt (RS) structure phase transition is interpreted as a signature of the semiconductor to metal transition for $\text{Zn}_{1-x}\text{Mn}_x\text{Se}$. The above interpretation is further corroborated by the observation of the disappearance of the longitudinal optical phonon at the pressure where the ZB to RS structure transition occurs. © 1999 American Institute of Physics. [S0021-8979(99)05312-8]

I. INTRODUCTION

The physical properties of semiconductors at high pressure have attracted a lot of attention. Tuchman *et al.*¹ found interesting photoluminescence (PL) behavior in $\text{ZnSe}/\text{ZnMnSe}$ superlattices under hydrostatic pressure. They concluded that the band alignment for the $\text{ZnSe}/\text{ZnMnSe}$ superlattice is type I. Faster increase in energy in the biexciton PL was observed. Gorczyca and Christensen² and Yamada and Masumoto³ studied the band-alignment-type conversion in the ZnS/ZnSe strained-layer superlattice. Ves *et al.* found that the band gap in ZnSe opens up as the applied pressure increases.⁴ Arora *et al.*⁵ reported the splitting of the transverse optical (TO) phonon at pressures around 2.8 and 5.2 GPa. Lee and Ihm theoretically studied the pressure-induced structure phase transition of ZnTe .⁶ Li *et al.* used a high-pressure technique to study the photoluminescence spectra of doped ZnSe for the identification of impurity locations.⁷ The pressure-induced metallization of ZnSe was observed by Itkin *et al.*⁸ Qadri *et al.*⁹ used energy-dispersive x-ray diffraction (EDXD) measurements to study the pressure-induced zinc blende (ZB) to rock salt (RS) (sodium chloride, NaCl) phase transition of $\text{Zn}_{0.83}\text{Fe}_{0.17}\text{Se}$ crystal. The transition from the zinc blende (B_3) to sodium chloride (B_1) phase was determined to be 10.4 ± 0.6 GPa.

Recently, we studied the phonon Raman scattering of ZnSe and ZnFeSe bulk crystals.^{10–12} The semiconductor to metal phase transition was found to coincide with the zinc blende to rock salt structural transition. At the transition pressure, the longitudinal optical (LO) phonon disappears in the Raman spectra due to the metallization of the ZnSe and ZnFeSe bulk crystals. At the transition pressure, the TO phonons are still observable in the Raman spectra due to the possible existence of transverse surface vibration modes. The physical properties of ZnMnSe bulk crystals are similar to those of ZnFeSe bulk crystals. Both types of crystals belong to the diluted magnetic semiconductor (DMS) family.¹³ However, to the best of our knowledge, pressure-induced structural transitions have not been studied at high pressure. In this article, the pressure-induced structural transitions of $\text{Zn}_{0.93}\text{Mn}_{0.07}\text{Se}$ and $\text{Zn}_{0.76}\text{Mn}_{0.24}\text{Se}$ bulk crystals were studied using energy-dispersive x-ray diffraction at pressures up to 25 GPa. The zinc blende to rock salt structural transitions were observed at 11.8 ± 1.5 and 9.9 ± 0.5 GPa. We propose that the pressure-induced zinc blende to rock salt structural transition is an indirect observation of the semiconductor to metal phase transition. In addition, the Raman scattering of the $\text{Zn}_{0.93}\text{Mn}_{0.07}\text{Se}$ and $\text{Zn}_{0.76}\text{Mn}_{0.24}\text{Se}$ bulk crystals were studied at high pressures up to 35 GPa.

II. EXPERIMENT

In the energy-dispersive x-ray diffraction experiments, crystals grown using the modified Bridgman method were

^{a)} Author to whom correspondence should be addressed. Electronic mail: pechou@phys730.cycu.edu.tw

ground into small particles of 1 μm in size. The samples were then loaded with gold powder into a Mao–Bell-type diamond anvil cell (DAC), which had two 1/3 carat diamonds and 600 μm culets. The gold powder was used for the calibration of the DAC pressure.¹⁴ The energy-dispersive x-ray diffraction experiments were carried out at the X17C beam line of the National Synchrotron Light Source (NSLS) of the Brookhaven National Laboratory (BNL). The beam size was $50 \times 50 \mu\text{m}^2$. A germanium energy-dispersive detector, which had 1024 channels was set in position, where the diffraction angle was 5° , for the detection of the diffracted x-ray beam. The spectrum resolution was about 0.1 keV, which corresponded to the accuracy of d_{hkl} (crystal-plane spacing) calculation of about $5 \times 10^{-3} \text{ \AA}$. The precision for the determination of the peak position of the diffraction x ray from 0.1 keV of gold powder corresponded to a resolution of DAC pressure of about 0.3–0.5 GPa. In cases of high-pressure Raman scattering, the ruby powder was loaded with samples for pressure calibration using the fluorescence scale method.^{15,16} The Raman spectra and the fluorescence spectra of ruby powders were obtained using a Renishaw 2000 micro-Raman system. The 514.5 nm line from the Coherent INNOVA 5.0 W Ar^+ laser is used as the excitation. Usually, a laser beam with a power of 80 mW was focused to a size of about 5 μm on the sample surface in the DAC. The back-scattering Raman signals were collected using the micro-Raman system and detected by a cooled Peltier charge-coupled device. To analyze the Raman spectra, a Jandel Scientific Peakfit Computer Program was used to calculate the position, intensity, and the width at the half maximum of the peaks. The spectral resolution was better than 2 cm^{-1} . As a result, the precision of the pressure determination, which was done by reading the peak position of the ruby R_1 and R_2 fluorescence, was much better than 0.5 GPa.

III. RESULTS AND DISCUSSION

The energy-dispersive x-ray diffraction spectra from the $\text{Zn}_{0.93}\text{Mn}_{0.07}\text{Se}$ bulk crystal, which had a ZB structure (B_3 phase) at ambient pressure, are shown in Fig. 1. At 2.6 GPa, the peaks at 22, 36, and 42 keV are attributed to the diffraction from the (111), (220), and (311) planes of the $\text{Zn}_{0.93}\text{Mn}_{0.07}\text{Se}$ bulk crystal, respectively, while the peak at 30 keV is identified as the diffraction from the (111) planes of gold used as the pressure calibration. The diffraction peak of the Au (200) planes at 35 keV was too weak to be observed. As the pressure is raised, the diffraction peaks exhibit a blueshift in energy due to the shortening of the lattice constant. At 10.8 GPa, additional peaks emerge at 27.7 and 40 keV. The two peaks are attributed to the diffraction of the (200) and (220) planes of the RS structure (B_1 phase) of $\text{Zn}_{0.93}\text{Mn}_{0.07}\text{Se}$. As the pressure is increased further, the diffraction due to the ZB structure disappears. The variation in plane spacing versus pressure for the (hkl) planes and the equation of state (EOS) V/V_0 versus pressure, are shown in Fig. 2 using solid circles and open squares, respectively. The spacing d_{hkl} between the (111) planes of the ZB structure (B_3 phase) was 3.26 \AA at ambient pressure. The plane spacing d_{111} decreases to 3.13 \AA as the pressure is increased to

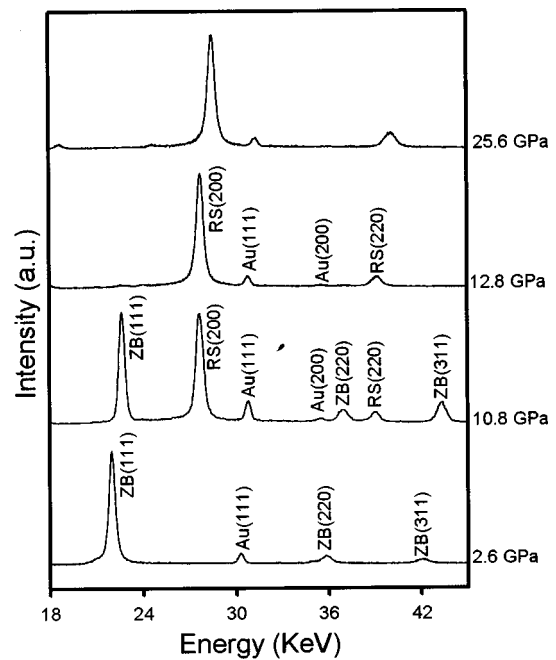


FIG. 1. Energy-dispersive x-ray diffraction spectra of $\text{Zn}_{0.93}\text{Mn}_{0.07}\text{Se}$ bulk crystal at various pressure. ZB denotes zinc-blende structure. While RS represents rock salt structure.

10.8 GPa. The volume decreases to about 89% of the initial volume (V_0), which was measured at ambient pressure. At the same pressure, the ZB (B_3 phase) to RS (B_1 phase) structure transition occurred. The sample volume dropped to about 75% of the original volume V_0 . As the pressure was increased further to 12.8 GPa, the diffraction peaks due to the ZB phase disappeared. Due to the difficulty in pressure tuning, no data point was obtained between 10.8 and 12.8 GPa. As a result, the ZB–RS (B_3 – B_1) phase transition pressure at which the crystal transform fully from ZB (B_3) to RS (B_1) should be written as 11.8 ± 1.5 GPa. The error bar of 1

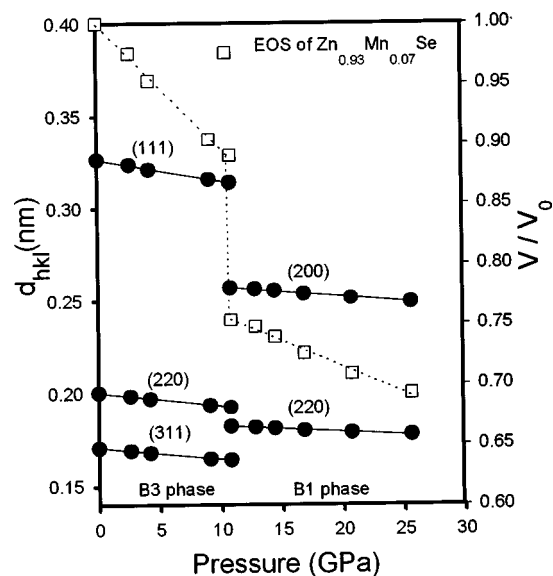


FIG. 2. Variation of plane spacing d_{hkl} and V/V_0 vs pressure for the $\text{Zn}_{0.93}\text{Mn}_{0.07}\text{Se}$ bulk crystal.

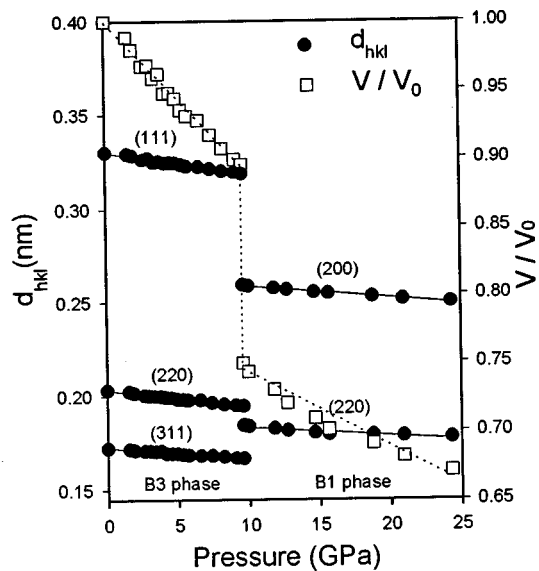


FIG. 3. Variation of plane spacing d_{hkl} and V/V_0 vs pressure for the $\text{Zn}_{0.76}\text{Mn}_{0.24}\text{Se}$ bulk crystal.

GPa results from the difficulty of pressure tuning while the error of 0.5 GPa comes from the uncertainty of the pressure determination. The bulk modulus evaluated at low pressure for $\text{Zn}_{0.93}\text{Mn}_{0.07}\text{Se}$ is about 61.8 ± 0.8 GPa, which is slightly smaller than that of 62.4 ± 0.8 GPa for ZnSe. This implies softening of the lattice due to the substitution of Zn by Mn. Note that the change in bulk modulus was only about 1%.

The variation of d_{hkl} for $\text{Zn}_{0.76}\text{Mn}_{0.24}\text{Se}$ with pressure is shown in Fig. 3. At ambient pressure, the plane spacings d_{111} , d_{220} , and d_{311} of the (111), (220), and (311) planes were 3.31, 2.03, and 1.72 Å, respectively. The plane spacing decreases with pressure due to the shortening of the lattice constant. Below 9.0 GPa, the crystal structure is ZB. At 9.8 GPa, the zinc blende to rock salt phase transition occurs. The volume drops from 89% of the initial volume V_0 to 75% of V_0 . Above 10.0 GPa, the diffraction due to the ZB phase disappears. For this sample, the pressure tuning was much better controlled. More data points were obtained in the neighborhood of the phase transition. As a result, the error bar is only 0.5 GPa, which was caused by the uncertainty in the pressure determination. The pressure where the crystal fully transforms from ZB to RS could be written as 9.9 ± 0.5 GPa.

In Fig. 4, the V/V_0 versus pressure of ZnSe, $\text{Zn}_{0.93}\text{Mn}_{0.07}\text{Se}$ and $\text{Zn}_{0.76}\text{Mn}_{0.24}\text{Se}$ crystals are shown using open circles, open squares, and open triangles, respectively. The ZnSe data were obtained from the previous work done by Greene, Luo, and Ruoff.¹⁷ The ZB–RS transition pressure drops from 15.5 ± 0.5 to 11.8 ± 1.5 GPa, and 9.9 ± 0.5 GPa for ZnSe, $\text{Zn}_{0.93}\text{Mn}_{0.07}\text{Se}$ and $\text{Zn}_{0.76}\text{Mn}_{0.24}\text{Se}$ crystals, respectively. The respective bulk modulus, which are evaluated at low pressure are 62.4 ± 0.8 , 61.8 ± 0.8 , and 60.5 ± 0.8 GPa. The drop in bulk modulus and the structural phase transition pressure are attributed to the softening of the lattice, which is caused by then replacement of Zn by Mn. For ZnSe there is a range, 12.2–15.5 GPa, where the zinc blende and rock salt structure coexists. In the case of $\text{Zn}_{0.93}\text{Mn}_{0.07}\text{Se}$, due to the

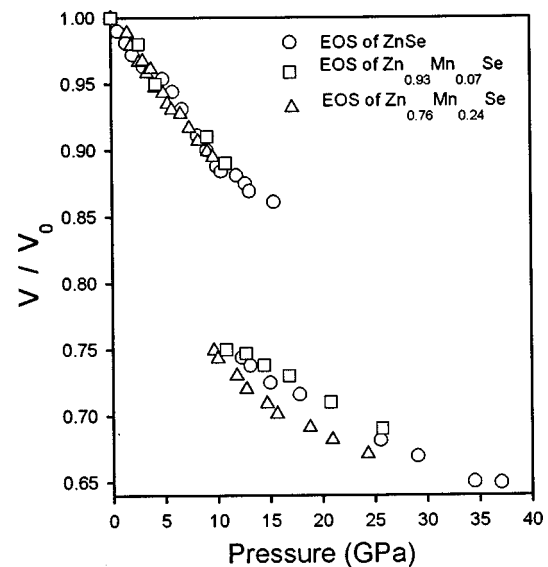


FIG. 4. V/V_0 vs pressure for ZnSe, $\text{Zn}_{0.93}\text{Mn}_{0.07}\text{Se}$, and $\text{Zn}_{0.76}\text{Mn}_{0.24}\text{Se}$ bulk crystals. The data points for ZnSe are obtained from Ref. 12.

difficulty in the fine pressure tuning, no data points were obtained between 9 and 11 GPa (also 11 and 13 GPa). While, in the case of $\text{Zn}_{0.76}\text{Mn}_{0.24}\text{Se}$ crystals, the pressure tuning was better controlled. At 9 GPa, only the ZB (B_3) phase was observed. Above 10 GPa, only the RS (B_1) phase was observed.

In Fig. 5, the Raman spectra from the $\text{Zn}_{0.76}\text{Mn}_{0.24}\text{Se}$ bulk crystal are shown at pressures up to 10.9 GPa. The dotted lines represent the numerical fit to the experimental data. At ambient pressure, three Raman peaks are observed. The LO phonon locates at 253 cm^{-1} , while the TO phonon is situated at 198 cm^{-1} . Between the TO and LO phonons, the

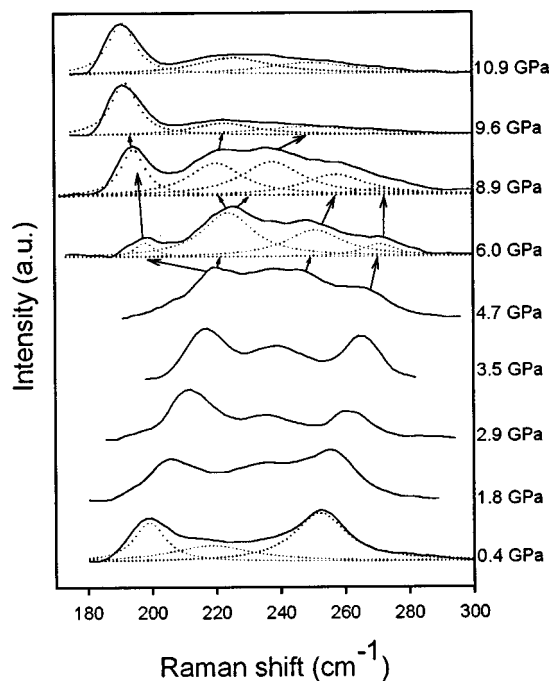


FIG. 5. Solid lines: Raman spectra of the $\text{Zn}_{0.76}\text{Mn}_{0.24}\text{Se}$ bulk crystal at various pressure. Dotted lines: numerical fit to the experimental data.

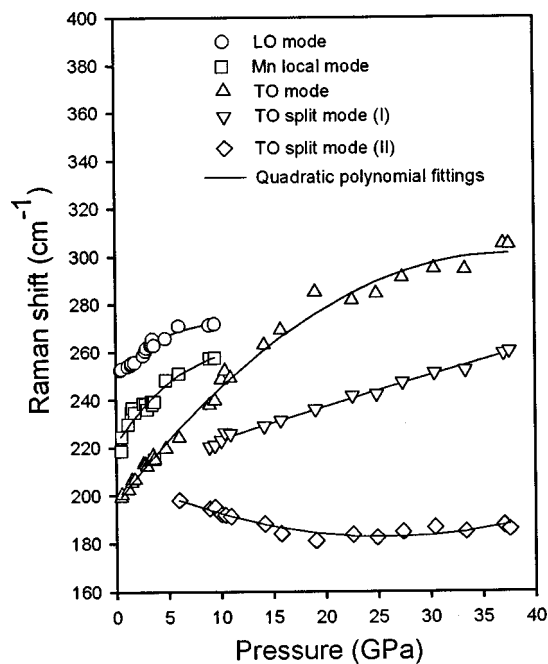


FIG. 6. Pressure dependence of the Raman shifts of the LO (circles), Mn local-mode (squares), TO (triangles), TO split I (inverted triangles), and TO split II (rhombi) for $Zn_{0.76}Mn_{0.24}Se$ bulk crystals. Solid lines are the quadratic polynomial fit to the experimental data.

Mn impurity mode is observed at 219 cm^{-1} . As the pressure is increased, all of the three phonon modes exhibit a blueshift. At pressure around 4.7 GPa, a split TO phonon mode starts to develop. It becomes very pronounced at 6.0 GPa. The split TO phonon mode exhibits a redshift in energy. The occurrence of splitting of the TO phonon mode implies a phase transition, which was reported by Arora *et al.*⁵ As the pressure is increased further, the TO phonon mode splits once more. The second splitting occurs at a pressure around 8.0 GPa. A summary plot of the Raman shift versus pressure of all the Raman peaks is shown in Fig. 6. The solid lines represent the quadratic fit to the data. For LO, the fit is represented by $248.9 + 4.05p - 0.173p^2\text{ cm}^{-1}$ (the unit of pressure is GPa). Above 9.6 GPa, the LO and Mn impurity modes become almost invisible. The same phenomena, disappearance of the LO and impurity mode, were observed in $ZnFeSe$ bulk crystal by us recently.¹⁰⁻¹² The disappearance of the LO and impurity mode is attributed to the semiconductor to metal phase transition. The phase transition pressure, 9.6 ± 0.5 GPa, is coincident with the ZB to RS structure transition pressure 9.9 ± 0.5 GPa, as shown in Fig. 4. At pressures above the phase transition, the samples become opaque. This implies that for ZnSe-based ternary compounds ($ZnMnSe$ and $ZnFeSe$), both the disappearance of the LO and impurity mode phonons and the ZB to RS structural transition are the signatures of the semiconductor to metal transition.

The high-pressure Raman spectra for the $Zn_{0.93}Mn_{0.07}Se$ bulk crystal are similar to that of the $Zn_{0.76}Mn_{0.24}Se$. The summary plot is shown in Fig. 7. It is clear that the Mn concentration dependence of the transition pressure is similar to the EDXD work, the transition pressure decreases with Mn concentration. For both $Zn_{0.93}Mn_{0.07}Se$ and

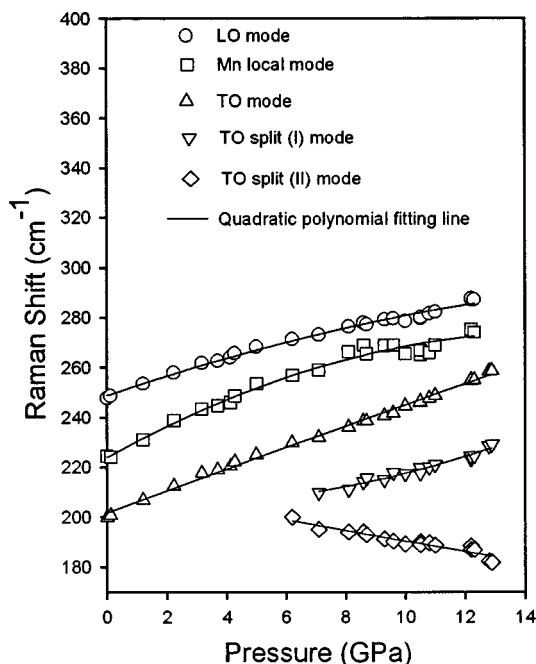


FIG. 7. Pressure dependence of the Raman shifts of the LO (circles), Mn local-mode (square), TO (triangles), TO split I (inverted triangles), and TO split II (rhombi) for $Zn_{0.93}Mn_{0.07}Se$ bulk crystals. Solid lines are the quadratic polynomial fit to the experimental data.

$Zn_{0.76}Mn_{0.24}Se$ bulk crystals, two TO split modes are observed at pressures below the ZB-RS (B_1-B_3) phase transition pressure. The splittings could result from the deformation of the crystals. The deformation breaks the crystal symmetry of the ZB (B_3) structure. This in turn results in the splitting of the TO phonon model. However, the evolution of the crystal deformation is not known. As the pressure exceeds the structural transition pressure, the fourfold covalent bonding of the ZB structure transforms into nondirectional ionic bonding of the RS structure, which has six nearest neighbors for both anions and cations. When the structural transition is complete, by compressing the lattice further, the interion distance of the RS lattice decreases. The decrease in the interion distance makes electron hopping between the anions relatively easy. As a result, the resistance of the semiconductor drops to a value comparable to that of metal. The corresponding pressure at which $Zn_{0.93}Mn_{0.07}Se$ and $Zn_{0.76}Mn_{0.24}Se$ crystals fully transform from the ZB to RS structure 11.8 ± 1.5 and 9.9 ± 0.5 GPa, respectively. We, therefore, propose that the occurrence of the ZB to RS structure and the disappearance of the LO and impurity mode phonon transition are signatures of the metallization of semiconductors.

IV. CONCLUSION

The pressure-induced structural phase transition of $Zn_{0.93}Mn_{0.07}Se$ and $Zn_{0.76}Mn_{0.24}Se$ bulk crystals were investigated using EDXD experiments. The calculated bulk moduli were 62.4 ± 0.8 , 61.8 ± 0.8 , and 60.5 ± 0.8 GPa for $ZnSe$, $Zn_{0.93}Mn_{0.07}Se$, and $Zn_{0.76}Mn_{0.24}Se$ bulk crystals, respectively. Indirect observation of the metallization of semiconductors was proposed. The pressure-induced metalliza-

tion for ZnSe, $\text{Zn}_{0.93}\text{Mn}_{0.07}\text{Se}$, and $\text{Zn}_{0.76}\text{Mn}_{0.24}\text{Se}$ crystals occurred at 15.5 ± 0.5 , 11.8 ± 1.5 , and 9.9 ± 0.5 GPa, respectively. The observed reduction in the structural transition pressure of ZnMnSe with Mn concentration implies that the replacement of Zn by Mn results in a decrease in the metallization pressure. This also indicates that the replacement of Zn by Mn results in softening of the crystal bonding and instability of the crystal structure.

ACKNOWLEDGMENTS

This work was supported by the National Science Council and Chung Yuan Christian University by Grant Nos. NSC-87-2613-M-213-008, NSC-87-2112-M-033-004, NSC-87-2112-M-033-007, NSC88-2112-M-033-003, and CY86-RG-001. One of the authors (W.C.C.) would like to thank the constant support from Professor Jiang and the Award of Distinguished Professor at Chung Yuan Christian University.

¹J. A. Tuchman, Z. Sui, S. Kim, and I. P. Herman, *J. Appl. Phys.* **73**, 7730 (1993).

²I. Gorczyca and N. E. Christensen, *Phys. Rev. B* **48**, 17202 (1993).

³Y. Yamada and Y. Masumoto, *Phys. Rev. B* **44**, 1801 (1991).

⁴S. Ves, K. Strossner, N. E. Christensen, C. K. Kim, and M. Cardona, *Solid State Commun.* **56**, 479 (1985).

⁵A. K. Arora, E. K. Suh, U. Debska, and A. K. Ramdas, *Phys. Rev. B* **37**, 2927 (1988); A. K. Arora and T. Sakuntala, *ibid.* **52**, 11052 (1995).

⁶G. Lee and J. Ihm, *Phys. Rev. B* **53**, R7622 (1996).

⁷M. Li, D. J. Strachan, T. M. Ritter, M. Tarmargo, and B. A. Weistein, *Phys. Rev. B* **50**, 4385 (1994).

⁸G. Itkin, G. R. Hearne, E. Sterer, and M. P. Pasternak, *Phys. Rev. B* **51**, 3195 (1995).

⁹S. B. Qadri, E. F. Skelton, A. W. Webb, N. Moulton, J. Z. Hu, and J. K. Furdyna, *Phys. Rev. B* **45**, 5670 (1992).

¹⁰C. M. Lin, D. S. Chuu, T. J. Yang, W. C. Chou, J. Xu, and E. Huang, *Phys. Rev. B* **55**, 13641 (1997).

¹¹C. M. Lin, D. S. Chuu, W. C. Chou, J. Xu, E. Huang, J. Z. Hu, and J. H. Pei, *Solid State Commun.* **107**, 217 (1998).

¹²C. M. Lin and D. S. Chuu, *Phys. Rev. B* **58**, 16 (1998); S. B. Qadri, E. F. Skelton, A. W. Webb, N. Moulton, J. Z. Hu, and J. K. Furdyna, *ibid.* **45**, 5670 (1992).

¹³J. K. Furdyna, *J. Appl. Phys.* **64**, R29 (1988).

¹⁴O. L. Anderson, D. G. Isaak, and S. Yamamoto, *J. Appl. Phys.* **65**, 1534 (1989).

¹⁵P. M. Bell, J. Xu, and H. K. Mao, in *Shock Waves in Condensed Matter*, edited by Y. M. Gupta (Plenum, New York, 1986), p. 125.

¹⁶J. Xu, H. K. Mao, and P. M. Bell, *Acta Phys. Sin.* **36**, 500 (1987).

¹⁷R. G. Greene, H. Luo, and A. L. Ruoff, *J. Phys. Chem. Solids* **56**, 521 (1995).